Title

Arachidonate-derived Dihomoprostaglandin Production Observed in Endotoxin-stimulated Macrophage-like Cells*

Journal

Journal of Biological Chemistry, 282(5)

ISSN

0021-9258

Authors

Harkewicz, Richard
Fahy, Eoin
Andreyev, Alexander
et al.

Publication Date

2007-02-01

DOI

10.1074/jbc.m610067200

Peer reviewed

THE JOURNAL OF BIOLOGICAL CHEMISTRY VOL. 282, NO. 5, pp. 2899–2910, February 2, 2007

Arachidonate-derived Dihomoprostaglandin Production Observed in Endotoxin-stimulated Macrophage-like Cells*[S]

Received for publication, October 27, 2006, and in revised form, November 17, 2006 Published, JBC Papers in Press, November 29, 2006, DOI 10.1074/jbc.M610067200

Richard Harkewicz[‡], Eoin Fahy[§], Alexander Andreyev[‡], and Edward A. Dennis[‡1]

From the [‡]Departments of Pharmacology, Chemistry, and Biochemistry, University of California, San Diego, La Jolla, California 92093-0601 and the [§]San Diego Supercomputing Center and University of California, San Diego, La Jolla, California 92093-0505

Eicosanoids, including the prostaglandins, leukotrienes, hydroxyeicosatetraenoic acids, epoxyeicosatetraenoic acids, and related compounds, are biosynthetic, bioactive mediators derived from arachidonic acid (AA), a 20:4(*n*-6) fatty acid. We have developed a comprehensive and sensitive mass spectral analysis to survey eicosanoid release from endotoxin-stimulated RAW 264.7 macrophage-like cells that is capable of detecting over 70 diverse eicosanoids and eicosanoid metabolites, should they be present. We now address the question: Are biologically significant eicosanoids being overlooked? Herein, we illustrate a general approach to diverse isotope metabolic profiling of labeled exogenous substrates using mass spectrometry (DIMPLES/MS), demonstrated for one substrate (AA) and its resultant products (eicosanoids). RAW cells were incubated in medium supplemented with deuterium-labeled AA. When the cells are stimulated, two sets of eicosanoids are produced, one from endogenous AA and the other from the supplemented (exogenous) deuterium-labeled form. This produces a signature mass spectral "doublet" pattern, allowing for a comprehensive and diverse eicosanoid search requiring no previous knowledge or assumptions as to what these species may be, in contrast to traditional methods. We report herein observing unexpected AA metabolites generated by the cells, some of which may constitute novel bioactive eicosanoids or eicosanoid inactivation metabolites, as well as demonstrating differing metabolic pathways for the generation of isomeric prostaglandins and potential peroxisome proliferator-activated receptor activators. Unexpectedly, we report observing a series of 1*a*,1*b*-dihomologue prostaglandins, products of adrenic acid (22:4(*n*-6)), resulting from the two-carbon elongation of AA by the RAW cells.

Starting in the early 1960s with the first structural characterization of the prostaglandins (1), mass spectrometry (MS)[2] has played a critical role in the biochemical study of eicosanoids. More recent advances in electrospray ionization-MS coupled to high-performance liquid chromatography have offered extremely sensitive and quantitative assays for most of the eicosanoids (2), without the need for chemical derivatization prior to analysis as was required by earlier gas chromatography electron ionization-MS methods (3). It is important to recognize, however, that while advances in high-performance LC-MS methods have offered extensive capabilities for surveying a number of different eicosanoid species in a single analysis, to date most efforts have focused on a specific eicosanoid or eicosanoid class, and additionally, with advanced knowledge and assumptions as to the identity of these species (4–11). Recently, however, investigators have begun to explore the development of theoretical databases and algorithms based on virtual liquid chromatography-UV spectroscopy-tandem mass spectrometry (MS/MS) spectra and chromatograms for identifying potential lipid mediators without synthetic or authentic products as standards (12).

Systems biology approaches include a comprehensive quantitative analysis of the manner in which all the components of a biological system interact functionally over time (13) and offer the promise of revolutionizing our understanding of cellular biology, personalized medicine, and drug design. A vital component of a systems biology approach is the global quantification of the spatial and temporal changes in lipid metabolites

* This work was supported by the LIPID MAPS Large Scale Collaborative Grant GM069338 from the U.S. National Institutes of Health. The costs of publication of this article were defrayed in part by the payment of page charges. This article must therefore be hereby marked "*advertisement*" in accordance with 18 U.S.C. Section 1734 solely to indicate this fact.

[S] The on-line version of this article (available at http://www.jbc.org) contains supplemental Table S1 and structures.

[1] To whom correspondence should be addressed: Depts. of Pharmacology, Chemistry and Biochemistry, University of California, San Diego, 9500 Gilman Drive, La Jolla, CA 92093-0601. Tel.: 858-534-3055; Fax: 858-534-7390; E-mail: edennis@ucsd.edu.

[2] The abbreviations used are: MS, mass spectrometry; AA, arachidonic acid (5*Z*,8*Z*,11*Z*,14*Z*-eicosatetraenoic acid); AA-d_8, deuterated-AA (octadeuterated AA, 5*Z*,8*Z*,11*Z*,14*Z*-eicosatetraenoic acid, 5,6,8,9,11,12,14,15-d_8); adrenic acid, 7*Z*,10*Z*,13*Z*,16*Z*-docosatetraenoic acid; COX, cyclooxygenase; DiHETE, dihydroxy-eicosatetraenoic acid; DIMPLES/MS, diverse isotope metabolic profiling of labeled exogenous substrates using mass spectrometry; HETE, hydroxyeicosatetraenoic acid; HpETE, hydroperoxyeicosatetraenoic acid; Kdo_2-Lipid A, (3-deoxy-D-*manno*-octulosonic acid)$_2$-Lipid A; LC-RT, liquid chromatography-retention time; MS/MS, tandem mass spectrometry; MRM, multiple reaction monitoring; PGD_2, prostaglandin D_2 (9*S*,15*S*-dihydroxy-11-oxo-5*Z*,13*E*-prostadienoic acid); PGE_2, prostaglandin E_2 (9-oxo-11*R*,15*S*-dihydroxy-5*Z*,13*E*-prostadienoic acid); $PGF_{2\alpha}$, prostaglandin $F_{2\alpha}$ (9*S*,11*R*,15*S*-trihydroxy-5*Z*,13*E*-prostadienoic acid); PGG_2, prostaglandin G_2 (9*S*,11*R*-epidioxy-15*S*-hydroperoxy-5*Z*,13*E*-prostadienoic acid); PGH_2, prostaglandin H_2 (9*S*,11*R*-epidioxy-15*S*-hydroxy-5*Z*,13*E*-prostadienoic acid); PGJ_2, prostaglandin J_2 (11-oxo-15*S*-hydroxy-5*Z*,8*Z*,13*E*-prostatrienoic acid); 11β-$PGF_{2\alpha}$ (9*S*,11*S*,15*S*-trihydroxy-5*Z*,13*E*-prostadienoic acid); 15d-$\Delta^{12,14}$-PGD_2, 15-deoxy-prostaglandin D_2 (11-oxo-9*S*-hydroxy-5*Z*,12*E*,14*E*-prostatrienoic acid); 15d-$\Delta^{12,14}$-PGJ_2, 15-deoxyprostaglandin J_2 (11-oxo-5*Z*,9,12E,14*Z*-prostatetraenoic acid); dihomoprostaglandin, 1*a*,1*b*-dihomologue prostaglandin; dihomo-PGD_2, dihomoprostaglandin D_2 (1*a*,1*b*-dihomo-9*S*,15*S*-dihydroxy-11-oxo-5*Z*,13*E*-prostadienoic acid); dihomo-PGE_2, dihomoprostaglandin E_2 (1*a*,1*b*-dihomo-9-oxo-11*R*,15*S*-dihydroxy-5*Z*,13*E*-prostadienoic acid); dihomo-$PGF_{2\alpha}$, dihomoprostaglandin $F_{2\alpha}$ (1*a*,1*b*-dihomo-9*S*,11*R*,15*S*-trihydroxy-5*Z*,13*E*-prostadienoic acid); dihomo-PGJ_2, dihomoprostaglandin J_2 (1*a*,1*b*-dihomo-11-oxo-15*S*-hydroxy-5*Z*,8*Z*,13*E*-prostatrienoic acid); dihomo- 15d-$\Delta^{12,14}$-PGD_2, dihomo-15-deoxyprostaglandin D_2 (1*a*,1*b*-dihomo-9*S*- hydroxy-11-oxo-5*Z*,12*E*,14*E*-prostatrienoic acid).

that occur with cellular metabolism, and no such strategy has yet to emerge. We have begun to address such a strategy using a single cell type, the RAW 264.7 macrophage-like cell, and a single stimulus, the high purity saccharolipid Kdo_2-Lipid A component of the endotoxin lipopolysaccharide (14) for the production of eicosanoids and their downstream metabolites. Specifically, a set of dose-response and time-course studies was carried out measuring eicosanoid release from Kdo_2-Lipid A-stimulated RAW cells. Eicosanoids[3] were detecting employing liquid chromatography coupled with MS and by operating the mass spectrometer in the ultrasensitive multiple reaction monitoring (MRM) mode, we had the capability to detect over 70 different eicosanoid and inactivation metabolite molecular species in a single analysis should they be present. Although this method does offer the capability for detecting a large number of diverse eicosanoid species, similarly it carries the limitations of the methods cited earlier (4–11); namely, that assumptions have to be made in advance regarding the species that might be present, to provide MRM pairs for the detection scheme. With our goal being to conduct a global survey of the eicosanoids produced by the stimulated RAW cells, we now address the question: Are biologically significant eicosanoids being overlooked? That is, are there species for which we have no prior knowledge of or expectation of their presence and, hence, no available MRM pairs that would be required for their detection?

In the present work, an MS-based general stable isotope exogenous substrate labeling strategy, which we coin "DIMPLES/MS" for diverse isotope metabolic profiling of labeled exogenous substrates using mass spectrometry, approaching a global metabolite survey is illustrated. Herein we demonstrate the DIMPLES/MS approach using one substrate, arachidonic acid (AA), and its RAW cell generated eicosanoids and related metabolites. RAW cells are incubated in medium supplemented with deuterium-labeled arachidonic acid (AA-d_8) and then stimulated with Kdo_2-Lipid A. Two sets of eicosanoid generation result, one set from endogenous AA, the other from the supplemented exogenous AA-d_8. This results in a "doublet" pattern, resolvable with mass spectrometry, allowing for a sensitive and comprehensive eicosanoid search without any previous knowledge or assumptions as to what these species may be, in contrast to traditional methods. Additionally, the AA-d_8-generated metabolites exhibit particular mass spectral patterns that may aid in determining possible functional groups and biosynthetic pathways, this being particularly useful when exploring for novel eicosanoids. Although DIMPLES/MS is demonstrated in this work for AA and eicosanoids, its utility should prove equally valuable for other substrates and the diverse analysis of their corresponding metabolites. Using DIMPLES/MS we report herein observing unidentified metabolic products of AA generated by Kdo_2-Lipid A-stimulated RAW cells, which have the potential for being novel eicosanoids. If these unidentified species do exhibit particularly interesting and biologically relevant properties, the labor-intensive work required to determine their specific molecular details can be undertaken. Additionally, this approach reveals different detailed biosynthetic pathways for isomeric prostaglandins produced in these cells. Unexpectedly and of particular interest, we report observing a number of 22-carbon 1*a*,1*b*-dihomologue prostaglandins (dihomoprostaglandins), products of adrenic acid (22:4(*n*-6)) resulting from the two-carbon elongation of AA by the RAW cells. Although previously it has been observed that adrenic acid can serve as a COX substrate when added to cells, resulting in the production of dihomoprostaglandins (15–17), there has been no demonstration of its formation *de novo* from an arachidonate precursor.

[3] For clarity, it should be noted that "eicosanoids" generally refer to the bioactive mediators derived from arachidonic acid and are active in the pico- to nanomolar range *in vitro* and *in vivo* (*i.e.* PGD_2, PGE_2, and $PGF_{2\alpha}$). These bioactive mediators can be further metabolized to inactive end products (*i.e.* 15-keto-PGE_2) and are then generally referred to as "metabolites of bioactive eicosanoids." For simplicity, in the present work both the bioactive mediators and their metabolites are occasionally referred to as "eicosanoids."

EXPERIMENTAL PROCEDURES

Materials—Dulbecco's modified Eagle's medium, penicillin/streptomycin, the Quant-iT DNA assay kit and the Vybrant Cytotoxicity assay kit were purchased from Invitrogen. Heat-inactivated fetal calf serum was purchased from HyClone (Logan, UT). Kdo_2-Lipid A (Lipid MAPS ID no. LMSL02000001; Avanti catalog no. 699500) was obtained from Avanti Polar Lipids (Alabaster, AL). All the standards used to compile our library of eicosanoid standards, including octa-deuterated AA (AA-d_8) used for supplementation, were purchased from Cayman Chemical (Ann Arbor, MI). Strata-X polymeric sorbent solid-phase extraction columns (catalogue no. 8B-S100-UBJ) were purchased from Phenomenex (Torrance, CA), and the vacuum manifold used with these extraction columns was purchased from Supelco (Bellefonte, PA). All reagents were chromatography grade and purchased from OmniSolv (Gibbstown, NJ).

Tissue Culture and AA-d_8 Supplementation—RAW 264.7 mouse macrophage-like cells were maintained in Dulbecco's modified Eagle's medium supplemented with 10% heat-inactivated fetal calf serum with low endotoxin content, 100 units/ml penicillin, and 100 μg/ml streptomycin in an incubator at 37 °C and 10% CO_2. 4×10^6 of these cells were plated in T-25 flasks with 4 ml of the same medium supplemented with and without 12.5 μg/ml (40 μM) of AA-d_8 for a 24-h period. Both sets of cells were then treated with 100 ng/ml of Kdo_2-Lipid A or an equivalent amount of Me_2SO-containing medium as a vehicle control for an additional 24 h. Thus four cell sample types were generated: Kdo_2-Lipid A treated with and without AA-d_8 supplementation and non-treated with and without AA-d_8 supplementation. The cultured medium from each set was then collected, centrifuged for 3 min at $1000 \times g$ to remove any floating cells, supplemented with 10% methanol, and subjected to an eicosanoid extraction procedure.

Eicosanoid/Fatty Acid Extraction Procedure—Solid-phase extraction of eicosanoids and fatty acids was performed using Strata-X polymeric sorbent columns connected to a vacuum manifold. Columns were pre-washed using 2 ml of methanol followed by 2 ml of water. Samples were loaded onto columns, washed with 2 ml of 90/10 water/methanol, then eluted with 1 ml of 100% methanol. The methanol was then evaporated to dryness using a SpeedVac, and the remaining sample was reconstituted with 100 μl of liquid chromatography buffer A.

Reversed-phase Liquid Chromatography—High-performance liquid chromatography was carried out using two Shimadzu (Columbia, MD) LC-10AD high performance pumps interfaced with a Shimadzu SCL-10A controller. Separation was performed using a 2.1- × 250-mm Vydac (Hesperia, CA) reversed-phase C_{18} column (catalogue no. 201TP52) equipped with a guard column (Vydac, catalogue no. 201GD52T) held at 35 °C. LC buffer A was water/acetonitrile/formic acid: 63/37/0.02, v/v; buffer B was acetonitrile/isopropanol: 50/50, v/v. Gradient elution was achieved using 100/0, A/B at 0 min and linearly ramped to 80/20, A/B by 6 min; linearly ramped to 45/55, A/B by 6.5 min and held until 11 min, linearly ramped to 28/72, A/B by 11.5 min and held until 16 min, then linearly ramped back to 100/0, A:B by 18 min and held there until 25 min to achieve column re-equilibration. In some cases (details listed later) a second gradient was employed using 100/0, A/B at 0 min and linearly ramped to 25/75, A/B by 16 min and held until 20 min, then linearly ramped back to 100/0, A:B by 22 min and held there until 30 min to achieve column re-equilibration. The buffer flow rate was 0.3 ml/min for both gradients. 10 and 30 μl of sample were injected onto the column using a Leap Technologies (Carrboro, NC) PAL autosampler. The liquid chromatography effluent was coupled to a mass spectrometer for further analysis.

Chiral Chromatography—Liquid normal phase chiral chromatography was carried out using the same pumping system described above for reversed-phase chromatography. Separation was carried out on a 4.6- × 250-mm Chiral Technologies (West Chester, PA) derivatized amylose column (Chiralpak® AD-H) equipped with a guard column (Chiralpak® AD-H guard column) held at 35 °C. Buffer A was hexane/anhydrous ethanol/water/formic acid: 96/4/0.08/0.02, v/v; buffer B was 100% anhydrous ethanol. This small amount of water in buffer A is miscible in the hexane/anhydrous ethanol mix and was found to be vital for satisfactory chiral separation and peak shape. Gradient elution was achieved using 100/0, A/B at 0 min and linearly ramped to 90/10, A/B by 13 min; linearly ramped to 75/25, A/B by 15 min and held until 25 min, then linearly ramped back to 100/0, A:B by 27 min and held there until 42 min to achieve column re-equilibration. The chiral chromatography effluent was coupled to a mass spectrometer for further analysis.

MS—All mass spectral analyses were performed using an Applied Bioscience (Foster City, CA) 4000 QTRAP hybrid triple quadrupole linear ion-trap mass spectrometer equipped with a Turbo V ion source and operated in full-scan, MS/MS, and multiple reaction monitoring (MRM) modes. Details regarding parameters specific to each mode of operation are provided below. For all experiments the Turbo V ion source was operated in negative electrospray mode (chiral chromatography utilized the ion source in chemical ionization mode; see below), and the QTRAP was set as follows: CUR = 10 p.s.i., GS1 = 40 p.s.i., GS2 = 40 p.s.i., IS = −4200 V, collisional activated dissociation = HIGH, TEM = 525 °C, ihe = ON, DP = −30 V, EP = −15 V and CXP = −10 V. The voltage used for collisional activated dissociation varied according to molecular species and ranged from −20 to −45 V.

The Turbo V ion source was operated in atmospheric pressure chemical ionization mode when employing chiral chromatography using the following settings: CUR = 10 p.s.i., GS1 = 45 p.s.i., GS2 = 60 p.s.i., NC = −3.0 μA, collisional activated dissociation = HIGH, temperature = 400 °C, ihe = ON, DP = −60 V, EP = −15 V, and CXP = −10 V.

Doublet Peak-picking Software—Raw mass spectral generated data files (ABI*.wiff) were acquired at an *m/z* resolution of 0.1 atomic mass unit and then converted to mzXML format (18) using the mzStar utility (www.sashimi.sourceforge.net/). The mzXML files were processed with a custom in-house program to integrate peaks in each full mass scan over a 0.6-atomic mass unit window and generate a formatted array of quantitated data for each mass spectral sample run. A set of customized Excel Visual Basic macros was then used to load a pair of array files (AA-d_8 supplemented and control), perform data normalization and subtractive analyses, view peaks of interest, and generate a list of detected mass spectral "doublets," according to user-defined criteria.

RESULTS

AA-d_8 Incorporation—A timeline depicting the supplementation of AA-d_8 to plated cells, Kdo_2-Lipid A stimulation, medium collection and extraction, and lastly LC-MS analysis is shown in Fig. 1*A*. The uptake of AA-d_8 by RAW cells as a function of time was determined by drawing an aliquot of medium from a plate of cells in 4 ml of medium supplemented with 12.5 μg/ml (~40 μM) AA-d_8 at 0, 0.5, 2, 5, and 18 h after initial supplementation, carrying out eicosanoid/fatty acid extraction, and measuring the relative amount of AA-d_8; this was also done for a sample identical to the above, however, containing no cells (control). A comparison of these two measurements permitted a determination of the amount of AA-d_8 remaining in the cell-containing medium at the different time periods, and the decrease could be attributed to uptake by the cells (Fig. 1*B*). LC-MRM-MS/MS (MRM pair of 311/267) was used to determine the relative amount of AA-d_8 in the medium, as defined by the area under its chromatographic peak, and its retention time was consistent with a standard. Triplicate samples were measured to determine the error shown in Fig. 1*B*. Note that at 18 h only a few percent of the initial AA-d_8 remained in the medium indicating that by the time of Kdo_2-Lipid A stimulation (after a 24-h incubation period) virtually all the AA-d_8 was incorporated into the cells.

AA/AA-d_8 Mass Spectral Doublet—The media from the four cell sample types (Kdo_2-Lipid A stimulation with and without AA-d_8 (control), and no stimulation with and without AA-d_8) were separately collected, extracted for eicosanoids/fatty acids, and resuspended in 100 μl of LC buffer A. A separate LC-MS analysis was performed for each, injecting 30 μl of sample onto the LC column and operating the mass spectrometer in full scan mode (*m/z* 280–400). The spectrum obtained for the stimulated/control sample (without AA-d_8) produced a number of peaks at various *m/z* values, most noticeably a very intense peak at *m/z* 351 accompanied by its C_{13} isotopic peaks at 352 and 353 (Fig. 2*A*, *solid line plot*) that had an LC retention time consistent with that of a prostaglandin D_2 (PGD_2) standard. The intensity of this peak was consistent with our previous Kdo_2-Lipid A

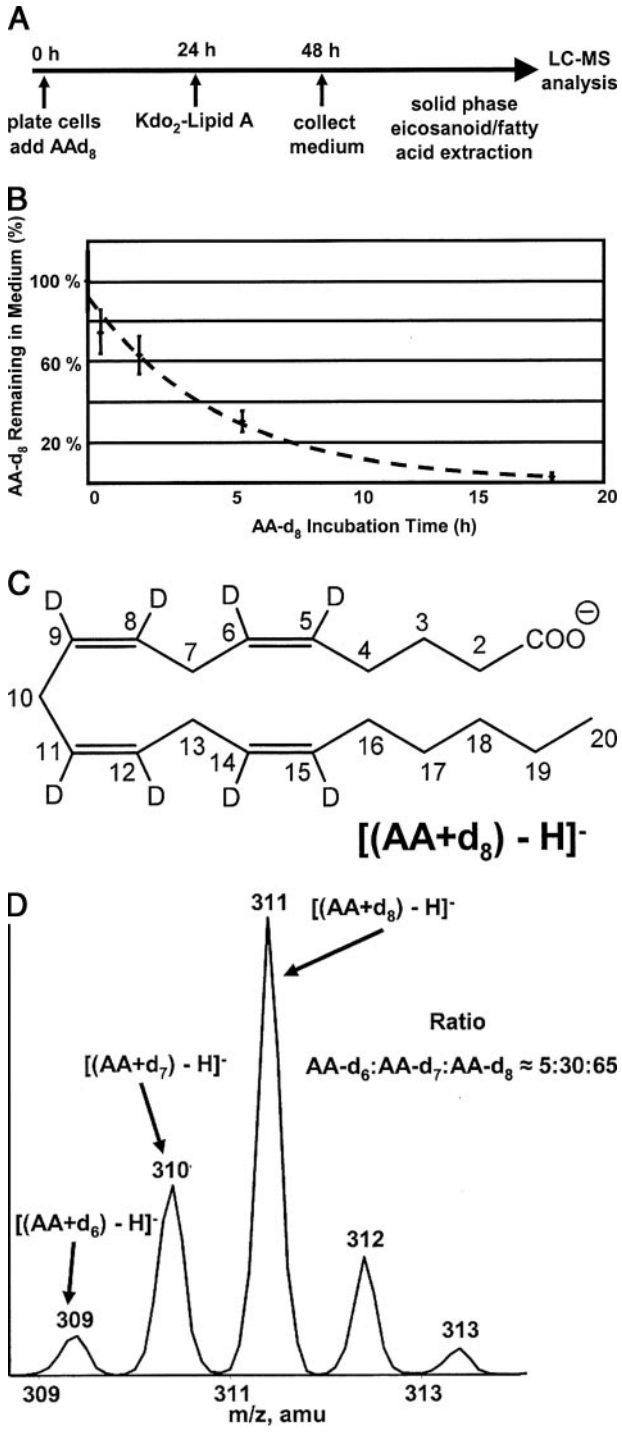

FIGURE 1. **AA-d_8 incorporation.** *A,* experimental timeline. AA-d_8 supplement (12.5 μg/ml, ~40 μM) was added to the medium at time of cell plating. After 24 h, the cells were treated with Kdo$_2$-Lipid A (100 ng/ml) for an additional 24-h period. Medium was then collected and subjected to a solid-phase eicosanoid/fatty acid extraction procedure, and the extracted products were analyzed using LC-MS. Note that, for a control sample, AA-d_8 supplementation and Kdo$_2$-Lipid A treatment were substituted with an equivalent amount of carrier solvent (ethanol or Me_2SO, respectively). *B*, plot of the measured amount of AA-d_8 remaining in cell culture medium as a function of time. Note that at 18 h only a few percent of the initial AA-d_8 remained in the medium, indicating its almost complete uptake by cells in this time period. *C*, molecular structure of deprotonated AA-d_8 and the location of its deuterium atoms. *D*, direct infusion full-scan mass spectral analysis of the AA-d_8 stock solution used for the supplementation in these experiments showing a portion of the molecules did not contain the maximal 8 deuterium atoms, but AA-d_7 and AA-d_6 was present in significant amounts as well in the ratio of ≈ 65%, 30 and 5%, respectively.

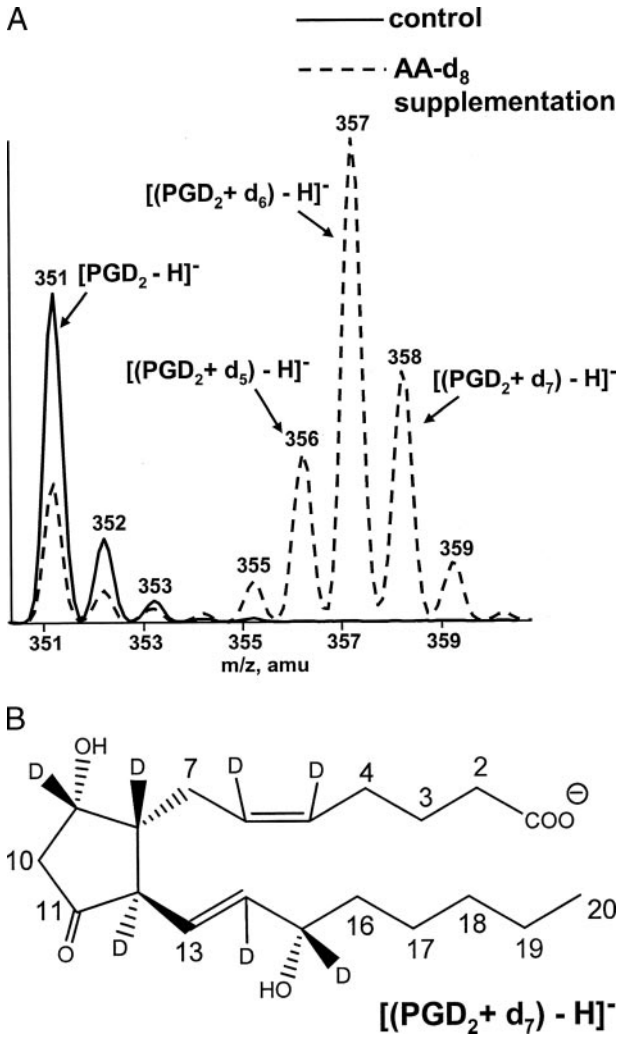

FIGURE 2. **AA/AA-d_8 mass spectral doublet.** *A*, recorded full scan mass spectra obtained from media extracts of Kdo$_2$-Lipid A-stimulated cells. Plot shows detection of prostaglandin D_2 (PGD_2) and overlay of two separately obtained data sets, with (*dashed line*) and without (control, *solid line*) AA-d_8 supplementation. The peak at *m/z* 351 is the deprotonated PGD_2 molecular ion, $(M\text{-}H)^-$, with its corresponding C_{13} natural abundance isotopic peaks at *m/z* 352 and 353. A mass offset pattern not present in the control sample is observed in the AA-d_8 supplemented sample, peaks offset higher by 4–8 atomic mass units from the peak at 351, corresponding to deprotonated PGD_2+d_6, PGD_2+d_6, and PGD_2+d_7 as labeled. The data are representative of three independent experiments. *B*, structure of deprotonated PGD_2+d_7 showing expected locations of deuterium atoms.

stimulated RAW cell results (14), in which PGD_2 has repeatedly been an eicosanoid produced in high abundance, typically 50–100 ng/10^6 cells.

A spectrum obtained for the stimulated/AA-d_8 sample (Fig. 2*A*, *dashed line plot*) contained peaks at *m/z* 351, 352, as 353 as before, but additionally a peak pattern offset 4–8 atomic mass units up from the 351 peak. Overlaying these two spectra (Fig. 2*A*) produces a conspicuous "doublet" pattern characterized by the peaks at 351, 352, and 353 present in both the AA-d_8 and control samples, and the higher offset peaks at 355–359 present only in the AA-d_8 sample and noticeably absent in the control sample. The higher offset peaks have a peculiar distribution shape, different from their non-deuterated counterpart, and we speculate that this is partly due to the actual number of deuterium atoms present on the deuterated-AA molecule used for

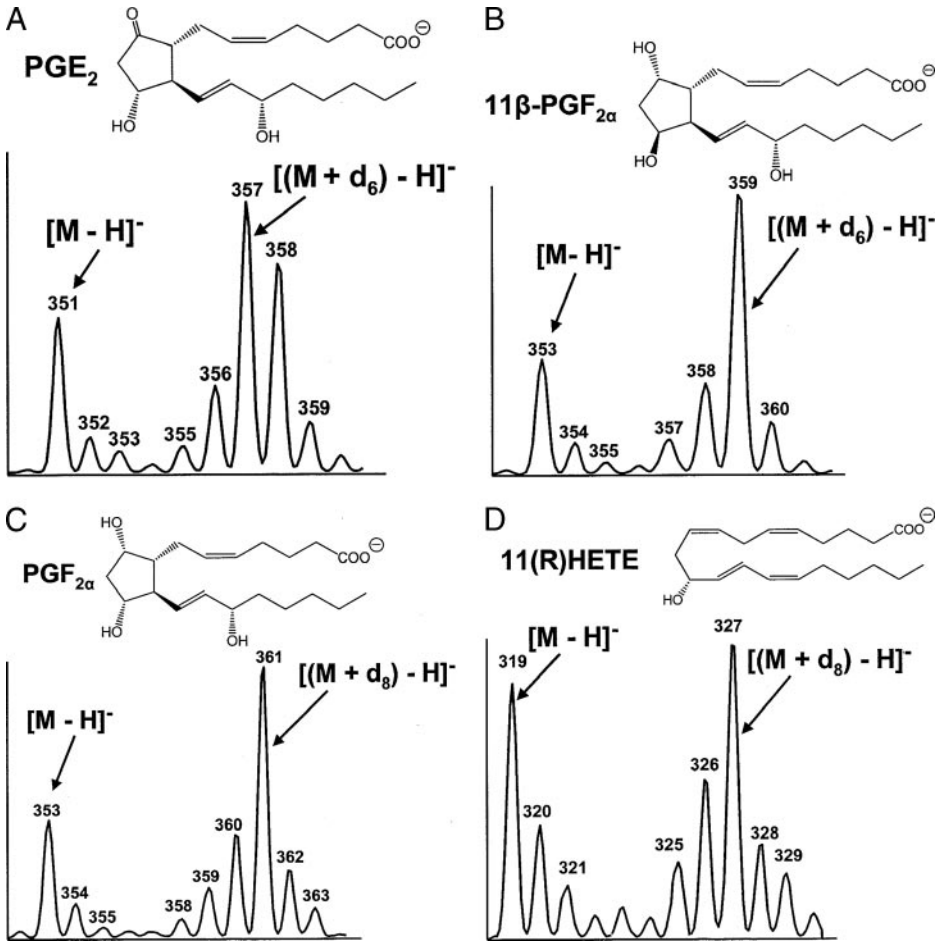

FIGURE 3. **Profiles of known eicosanoids produced by the AA-d_8-supplemented, Kdo_2-Lipid A-stimulated cells.** *A–D*, profiles extracted from an LC full scan mass spectral analysis for typical examples of eicosanoids produced by the AA-d_8-supplemented, Kdo_2-Lipid A-stimulated cells. These data are representative of three independent experiments.

supplementation; Fig. 1*C* shows the molecular structure of deprotonated AA-d_8 and the location of its deuterium atoms. A direct-infusion (sample was not run through an LC column) mass spectral analysis of the AA-d_8 stock solution used for the supplementation shows a portion of the molecules contained not only the maximal 8 deuterium atoms, but 7 (AA-d_7) and 6 (AA-d_6) as well in the ratio of ~65%, 30, and 5%, respectively (Fig. 1*D*). This ratio was determined using the integrated area under the three peaks, and any C_{13} contribution was ignored in this estimation. It is additionally noted that when the deuterated-AA was placed in cell medium (with serum) for a 48-h period, this produced no noticeable change in its deuterium atom containing distribution (data not shown).

It is important to note that, while the majority of the supplemented deuterated AA contains 8 deuterium atoms, the majority of the generated PGD_2 contains 6 deuterium atoms (PGD_2+d_6, m/z = 357, Fig. 2*A*). The formation of a ketone group on C-11 of PGD_2 (Fig. 2*B*) requires the loss of a deuterium atom from this position of its AA-d_8 precursor (Fig. 1*C*); however, because the peak at m/z = 357 in Fig. 2*A* (PGD_2+d_6) is so strongly present it is likely that another deuterium atom is being lost from AA-d_8 during its conversion into PGD_2, *i.e.* from C-8, C-12, C-15, or any of the other four remaining locations. It should be noted, however, that, because the peak at m/z 358 in Fig. 2*A* is present at a higher level than can be accounted for solely from a C_{13} isotopic contribution, PGD_2+d_7 is also formed (if the peak at m/z = 358 was solely due to a C_{13} contribution one would expect its intensity to be ~20% the intensity observed in the peak at m/z = 357). Therefore, the loss of this second deuterium atom appears to not be an absolute occurrence, as is the C-11 deuterium atom loss, but a loss that occurs a *significant* portion of the time during the AA-d_8 conversion to PGD_2.

Comparison of the two non-stimulated cell sample types (with/without AA-d_8 supplementation) shows a similar pattern as described above, the doublet pattern in the AA-d_8-supplemented sample compared with a major single peak at m/z 351, accompanied by its C_{13} isotopic peaks, in the non-supplemented sample. These were at basal levels in both samples, roughly 100-fold below stimulated intensity levels, a trend that has been previously observed (14). This would indicate that the AA-d_8 supplementation *per se* does not noticeably up-regulate eicosanoid production in the cell.

Fig. 3 (*A–D*) shows the profiles generated during an LC-full mass scan for some of the other known eicosanoids produced by the AA-d_8 supplemented, Kdo_2-Lipid A-stimulated cells. It should be noted that for some of these metabolites (*i.e.* $PGF_{2\alpha}$ and 11-HETE) the most abundant AA-d_8-generated products contain 8 deuterium atoms, whereas for others (PGD_2, PGE_2, and 11β-$PGF_{2\alpha}$) 6 deuterium atoms are contained in the most abundant product. The significance of these differences is addressed under "Discussion." Chiral chromatography (19) coupled to MRM mass spectrometry showed the 11-HETE species to be exclusively 11(*R*)-HETE (Fig. 4, *A* and *B*).

AA/AA-d_8 Doublet Recognition Software—In-house customized software has been developed for efficiently processing and comparing control and AA-d_8-supplemented mass spectral data sets for the entire liquid chromatography retention time (LC-RT) period and m/z range. To filter low level chemical noise, minimum threshold values for the AA control peak $(M-H)^-$ and the most intense of the deuterium atom containing peaks ([M-H]+d_5, [M-H]+d_6, [M-H]+d_7, and [M-H]+d_8) can be selected. A graphical display (Fig. 5*A*) provides an overlay of control (*black*) and AA-d_8 (*gray*) profiles corresponding to a selected LC elution time. The slider tool can be set to automatically step through the entire LC-RT range (0–16 min), dis-

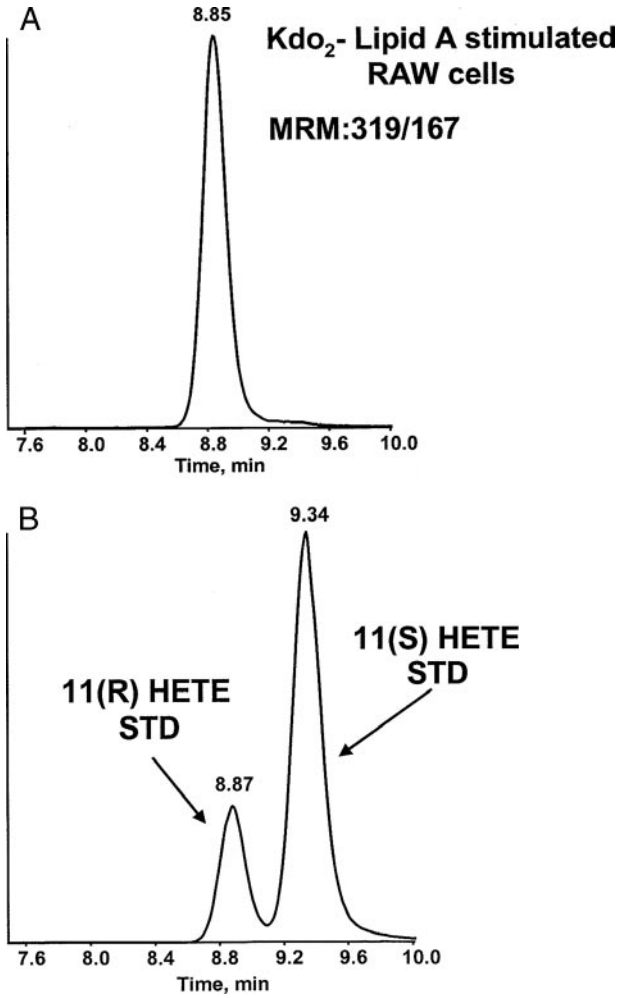

FIGURE 4. **Chiral chromatography confirms exclusive 11(*R*)-HETE production.** *A*, chiral chromatography coupled to MRM mass spectrometry showed the 11-HETE species produced by the Kdo_2-Lipid A-stimulated RAW cells to be exclusively 11(*R*)-HETE. *B*, chiral separation obtained running a mixture of 11(*R*)-HETE and 11(*S*)-HETE standards at a ratio of ~1:3 in concentration, respectively.

playing changing AA/AA-d_8 profiles with elution time. The program generates a table that provides quantitative information on these parameters. In summary, the software processes raw data and tabulates an AA/AA-d_8 doublet "hit" list according to a set of criteria as follows. Minimum intensity values are set for (i) the $(M\text{-}H)^-$ peak, (ii) the $\max([M\text{-}H]+d_{5,6,7,8})^-$ peak, (iii) the ratio of $\max([M\text{-}H]+d_{5,6,7,8})^-$ peak to the corresponding non-deuterated control peak. In the example shown in Fig. 5*A*, the $([M\text{-}H]+d_8)^-$, having an *m/z* of 389, is the most abundant of the deuterated-AA-supplemented peaks, and comparing it to the intensity of the *m/z* 389 background signal from the control yields a ratio of 53. The program also performs a correction for the tendency of the deuterated eicosanoids to elute slightly earlier than the corresponding non-deuterated molecules; ≈3–5 s under these chromatographic conditions.

AA/AA-d_8 Doublet Recognition of an Unidentified, Unknown Compound—Data sets collected from supplemented and non-supplemented (control) Kdo_2-Lipid A-stimulated RAW cell samples were processed using the software and a hit list was generated (Table 1, discussed below). One of the hits was a species with *m/z* of 381 and LC-RT of ~6.5 min (Fig. 5*A*), which did not match any entry in our "Library of Eicosanoid Standards" (Table 2). We have compiled a comprehensive library of eicosanoid standards, which is available in the supplemental material. The library contains information on each standard listed in Table 2 that includes LC-RT, systematic nomenclature and LIPID MAPS ID number (20), and an MS/MS fragmentation spectrum. If other reversed-phase liquid chromatography conditions are employed, these retention times can still be useful, because the order of elution should not drastically change; *e.g.* PGE_2 elutes prior to PGD_2 and 15-HETE elutes prior to 11-HETE, which elutes prior to 5-HETE. An overlay of the corresponding full-scan mass spectra obtained for the *m/z* of 381 metabolite discussed above is shown in Fig. 5*B*.

Tandem Mass Spectral Analysis of an Unidentified, Unknown Compound—Having recognized an unidentified, unknown compound at *m/z* 381 and LC-RT ≈ 6.5 m, a tandem mass spectrum (collision energy of −40 V) was obtained and is shown in Fig. 5*C*. The fragment ions observed in the MS/MS spectrum are used to generate MRM pairs, allowing the mass spectrometer to be operated in a highly sensitive detection mode. An 18-atomic mass unit loss from the parent ion $(M\text{-}H)^-$ is typically indicative of a water loss (hydroxyl group). Note the fragment peaks at 363, 345, and 327 in Fig. 5*C* suggesting the possibility of 3-hydroxyl groups contained on the parent ion. Interpretation of this spectrum is addressed in more detail under "Discussion."

Recognized Unknowns—A number of other hits were identified using our AA/AA-d_8 doublet recognition software for which there were no matches, based on *m/z* and LC-RT, in our eicosanoid library. A tandem mass spectrum was obtained for each of these unknowns, and similarly this information was used to generate MRM pairs. A partial list of these unknowns, including their most intense product ions and LC retention times, are listed in Table 1. Care was taken to ensure these species were not simply known compounds with water loses or adducted ions.

Some of the compounds listed in Table 1 were initially considered unidentified, however, upon further examination these were determined to be COX products of adrenic acid (22:4(*n*-6)), with the adrenic acid apparently resulting from the two-carbon elongation of AA by the RAW cells. The presence of deuterated adrenic acid and adrenic acid products (Fig. 6, *A* and *B*) strongly suggests their arachidonate origin. The tentative identities of these dihomoprostaglandins are listed in Table 1 (synthetic standards and additional approaches will be used to verify their identities). This unexpected and particularly interesting result is discussed in further detail below.

Semi-quantitative Comparison of AA, Adrenic Acid, and Their Products—The full-scan mass spectra obtained for AA, adrenic acid, and their products permitted a semi-quantitative comparison of these species. The intensity of product was obtained by integrating the area under the mono-isotopic parent ion ($[M\text{-}H]^-$) peak in full-scan mass spectra. To determine if this measurement was appropriately correlated to product amount, equal molar amounts of $PGF_{2\alpha}$ and dihomo-$PGF_{2\alpha}$ standards were loaded onto the reversed-phase liquid chromatography column, and it was observed that the areas corresponding to their mono-isotopic parent ion peak in their full-

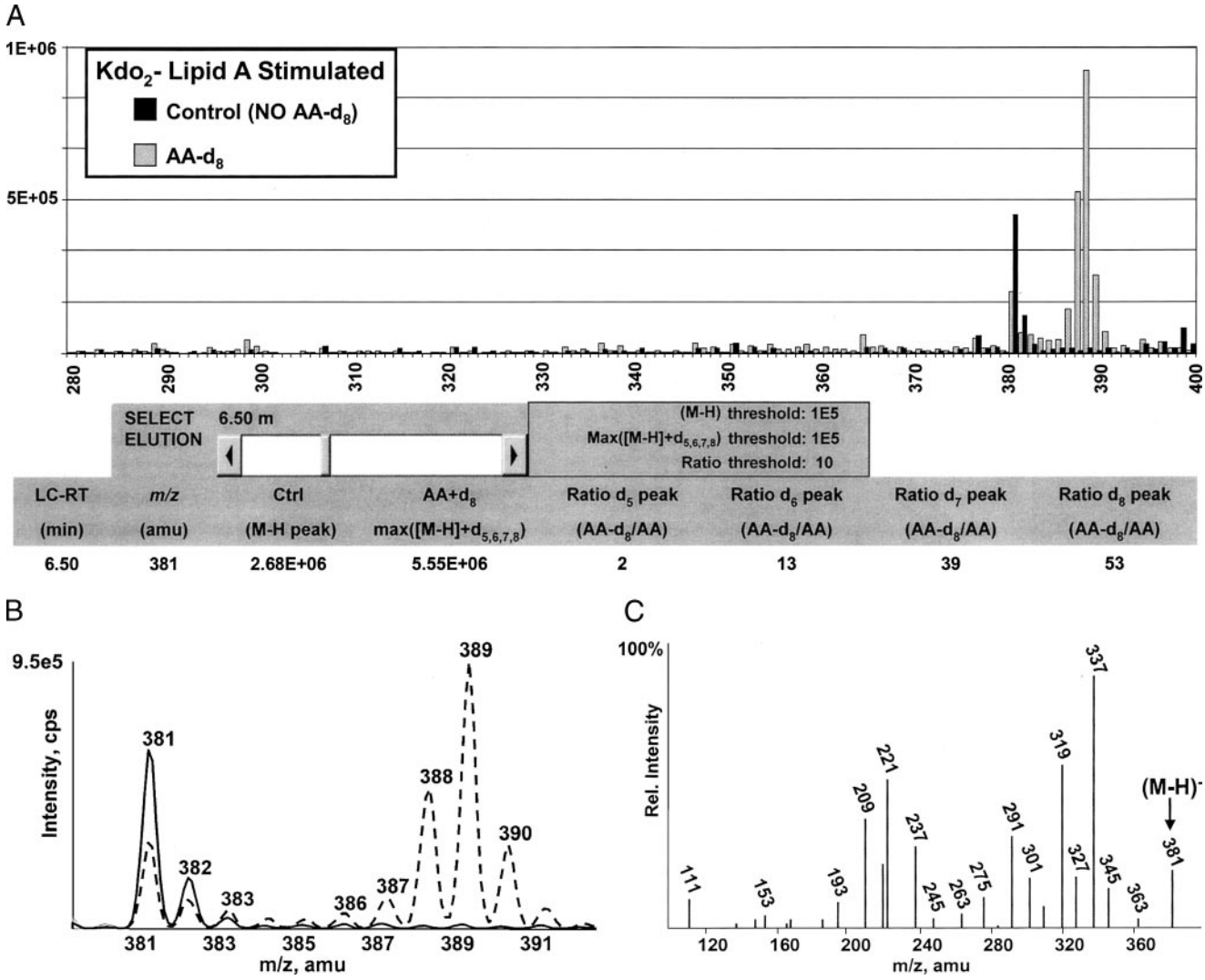

FIGURE 5. **AA/AA-d_8 doublet recognition software.** *A,* AA/AA-d_8 peak recognition software has been developed for efficiently processing and comparing control and AA-d_8 supplemented data sets for the entire liquid chromatography retention time (LC-RT) period and *m/z* range. Threshold values can be adjusted; additionally, $(M-H)^-$ must be greater than $([M+1]-H)^-$ to avoid selecting C_{13} isotopic peaks. A graphical display provides an overlay of control (*black*) and AA-d_8 (*gray*) profiles according to a selected LC elution time. The *table* provides a summary of quantitative measurements (refer to text for more detail). The example shown here provides results for a species with *m/z* of 381 and LC-RT of 6.5 m, which did not match any standard in our library, thus providing an indication of an "unknown" and potentially novel eicosanoid. *B*, corresponding overlay of full scan mass spectra obtained for stimulated RAW cell samples; control (*solid line*) and AA-d_8 (*dashed line*). The data are representative of three independent experiments. *C*, MS/MS spectrum obtained for fragmentation of $(M-H)^-$.

TABLE 1
MS/MS data of unidentified compounds

Unidentified compound[a]	*m/z* of $(M-H)^-$	Primary product ions						CE	LC-RT
								V	*min*
UNK 353-1	353	223	209	183	253	261		−30	5.2
UNK 381-1 (dihomo-$PGF_{2\alpha}$)[b]	381	337	221	319	209	237		−40	6.5
UNK 379-1 (dihomo-PGE_2)[b]	379	299	217	261	203			−45	6.8
UNK 379-2 (dihomo-PGD_2)[b]	379	299	217	261	203			−45	7.4
UNK 335-1	335	223	113	191	235	123	273	−30	8.0
UNK 361-1 (dihomo-PGJ_2)[b]	361	299	217	245	231			−35	9.4
UNK 335-2	335	273	205					−30	10.3
UNK 361-2 (dihomo-15d-$\Delta^{12,14}$-PGD_2)[b]	361	299	245	231				−35	10.5
UNK 347-1 (dihomo-11(*R*)-HETE)[b]	347	195	177					−35	13.7

[a] A partial list of unidentified compounds (unknown, UNK) in order of increasing LC-RT exhibiting AA/AA-d_8 doublets and flagged using AA/AA-d_8 doublet recognition software. Based upon *m/z* and LC-RT, none match any known compound in our eicosanoid library (Table 2). Primary product ions are listed for each unknown in descending order of intensity, determined through tandem mass spectral analysis (CE used is listed).

[b] Initially unidentified compounds were later determined to be cyclooxygenase products of adrenic acid (22:4(*n*-6)) and tentatively identified as specific dihomoprostaglandins, resulting from the two-carbon elongation of AA (20:4(*n*-6)) at the carboxyl end by the RAW cells. Refer to text for more details.

scan mass spectra were indeed similar (within 10%). A semi-quantitative comparison of AA, adrenic acid, and their corresponding products obtained from Kdo_2-Lipid A-stimulated RAW cells is shown in Fig. 7 The number above each pair is the ratio of adrenic acid to AA (products). It should be noted that no dihomo-15d-$\Delta^{12,14}$-PGJ_2 was observed.

TABLE 2
Eicosanoid standards library

Standard	$[M-H]^-$
12(*S*)-HHTrE	279
AA	303
AA-d_8	311
15d-$\Delta^{12,14}PGJ_2$	315
5-OxoETE	317
12-OxoETE	317
15-OxoETE	317
20-HETE	319
5(*R*)-HETE	319
5(*S*)-HETE	319
8(*R*)-HETE	319
8(*S*)-HETE	319
11(*R*)-HETE	319
11(*S*)-HETE	319
12(*R*)-HETE	319
12(*S*)-HETE	319
15(*R*)-HETE	319
15(*S*)-HETE	319
±5,6-EpETrE	319
±8,9-EpETrE	319
±11,12-EpETrE	319
±14,15-EpETrE	319
Tetranor PGEM	327
5(*S*)-HETE-d_8	327
Tetranor PGFM	329
PGA_2	333
PGB_2	333
PGJ_2	333
$\Delta^{12}PGJ_2$	333
dhk-PGA_2	333
Bicyclo-PGE_2	333
5(*S*),6(*R*)-DiHETE	335
5(*S*),6(*S*)-DiHETE	335
5(*S*),15(*S*)-DiHETE	335
8(*S*),15(*S*)-DiHETE	335
LTB_4	335
5(*S*)-HpETE	335
12(*S*)-HpETE	335
15(*S*)-HpETE	335
±5,6-DiHETrE	337
±8,9-DiHETrE	337
±11,12-DiHETrE	337
±14,15-DiHETrE	337
2,3-Dinor TXB_4	341
15-Keto-PGE_2	349
PGK_2	349
PGD_2	351
PGE_2	351
PGH_2	351
dhk-PGD_2	351
dhk-PGE_2	351
15-Keto-$PGF_{2\alpha}$	351
5(*S*),6(*R*),15(*S*)-LXA_4	351
5(*S*),6(*S*),15(*S*)-LXA_4	351
5(*S*),14(*R*),15(*S*)-LXB_4	351
$PGF_{2\alpha}$	353
11β-$PGF_{2\alpha}$	353
$PGF_{2\beta}$	353
dhk-$PGF_{2\alpha}$	353
PGD_2-d_4	355
PGE_2-d_4	355
$PGF_{2\alpha}$-d_4	357
PGG_2	367
19(*R*)-Hydroxy-PGE_2	367
20-Hydroxy-PGE_2	367
6-Keto-PGE_1	367
11-Dehydro-TXB_2	367
TXB_2	369
6-Keto-$PGF_{1\alpha}$	369
Diketodihydro-$PGF_{1\alpha}$	369
PGD_2-EA	394
PGE_2-EA	394
$PGF_{2\alpha}$-EA	396
LTE_4	448
LTC_4	624

DISCUSSION

DIMPLES/MS and Unexpected Metabolites—A strategy has been described for diverse isotope metabolic profiling of labeled substrates using mass spectrometry (DIMPLES/MS), devoid of any previous knowledge and assumptions as to what these metabolites may be. Details are provided by using deuterium-labeled AA (AA-d_8) and profiling its eicosanoid metabolites, however, we believe this strategy can be extended to other labeled exogenous substrates and their metabolic products.

When RAW macrophage-like cells are incubated in medium supplemented with AA-d_8, over time the endogenous fatty acids esterified to the *sn*-2 position of cell membrane glycerophospholipids are exchanged for the exogenous deuterated AA analog, however it appears that the endogenous AA is not completely replaced. When the cells are subjected to stimulation by lipopolysaccharide-like Kdo_2-Lipid A, our results show that the incorporated AA-d_8 behaves in a similar fashion to the endogenous AA of the cell, a cascade commences with the activation of phospholipase A_2, which hydrolyzes the *sn*-2 acyl ester bond resulting in a non-indiscriminating release of both free AA and AA-d_8. Both can then act as substrates for downstream enzymes, as is demonstrated by the production of PGD_2 and $PGD_2+[d_{5-7}]$ (Fig. 2*A*) as well as other known eicosanoids (Fig. 3, *A–D*), producing a conspicuous doublet pattern that is both observable with mass spectrometry and amenable to efficient processing of data sets using customized recognition software. Unexpectedly, dihomoprostaglandins, COX products of adrenic acid (22:4(*n*-6)), were also observed to be produced by the stimulated RAW, cells and a more detailed discussion regarding this finding is provided at the end of this section.

DIMPLES/MS Reveals Differing Mechanistic Origins and Metabolic Pathways of Isomeric Prostaglandins—The full scan mass spectral peak patterns generated with the AA-d_8-supplemented samples can provide insight into the origins of AA-derived metabolites and also into details on their molecular structures. An example of this is demonstrated with the different peak patterns observed for 11β-$PGF_{2\alpha}$ and $PGF_{2\alpha}$ (Fig. 3, *B* and *C*, respectively). Although these two compounds are stereoisomers of one another having identical fragmentation patterns (fortunately, 11β-$PGF_{2\alpha}$ has a shorter LC-RT than $PGF_{2\alpha}$ allowing them to be resolved in our analysis), they have significantly different origins. 11β-$PGF_{2\alpha}$ is an enzymatic product of PGD_2 (action of PGD_2 11-ketoreductase), whereas $PGF_{2\alpha}$ forms directly from PGH_2 (action of PGH_2 9,11-endoperoxide reductase) (21). The peak pattern observed for 11β-$PGF_{2\alpha}$, with $([M+d_6]-H)^-$ being the most intense peak of the deuterated components and resembling the pattern obtained for PGD_2 (Fig. 2*A*), supports that it does indeed originate from PGD_2. The peak pattern observed for $PGF_{2\alpha}$ is markedly different, with $([M+d_8]-H)^-$ being the most intense peak of the deuterated components. Originating directly from PGH_2 requires no deuterium loss at C11; a loss that is required if it were to originate from PGD_2 and discussed earlier. The mechanism for the formation PGE_2 (Fig. 2*A*) is similar to that for PGD_2 except the deuterium atom loss associated with the pentane ring ketogroup occurs at C9 instead of C11 and, here too, for PGE_2 the

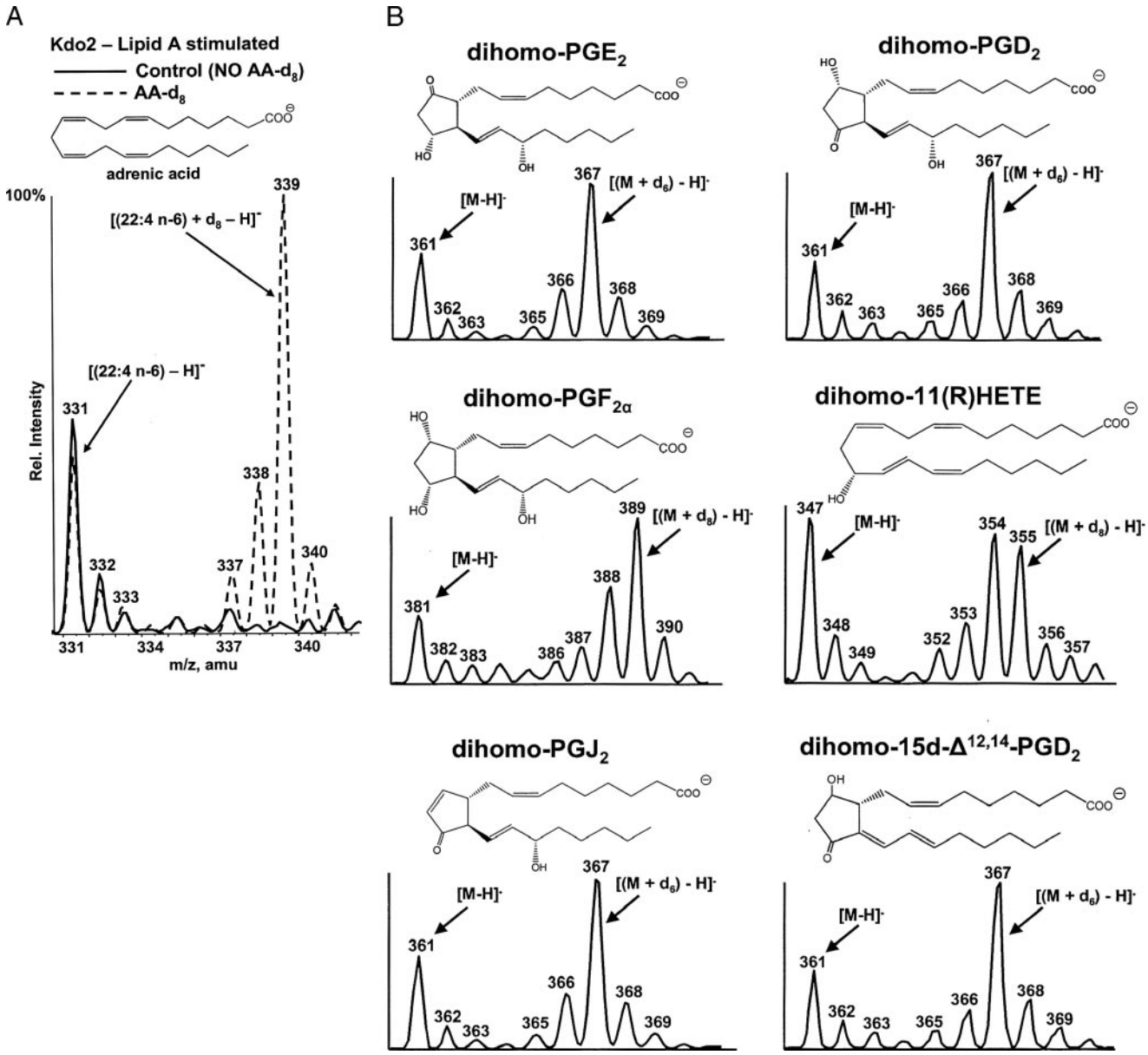

FIGURE 6. **Detection of arachidonate-derived dihomoprostaglandins.** *A*, full scan mass spectra obtained from media extracts of Kdo_2-Lipid A-stimulated cells showing detection of adrenic acid (22:4(*n*-6)) and overlay of two separately obtained data sets, with (*dashed line*) and without (control, *solid line*) AA-d_8 supplementation. *B*, profiles extracted from an LC full-scan mass analysis for tentatively identified dihomoprostaglandins produced by the AA-d_8-supplemented, Kdo_2-Lipid A-stimulated cells and a result of the two-carbon elongation of AA at its carboxyl end. $[M-H]^-$ is the endogenously produced peak, and $[(M+d^*)-H]^-$ is the most intense peak produced as a result of the AA+d_8 supplementation. The presence of deuterated adrenic acid and adrenic acid products strongly suggests their arachidonate origin. The data are representative of three independent experiments.

most intense peak of the deuterated components occurs with $([M+d_6]-H)^-$.

As stated earlier, chiral chromatography showed the 11-HETE produced by the RAW cells to be exclusively 11(*R*)-HETE (Fig. 4, *A* and *B*). It has been reported that 11(*R*)-HETE is an *abortive* COX product, resulting from the AA-to-prostaglandin G_2 pathway (see below) terminating before completion. It should also be noted that 11(*R*)-HETE (*no 11(S)-HETE*) would be the exclusive product of this termination process. Fig. 3*D* shows the full mass scan peak pattern for 11(*R*)-HETE generated from an AA-d_8-supplemented, Kdo_2-Lipid A-stimulated sample. Here, as with $PGF2_\alpha$, $([M+d_8]-H)^-$ is the most intense peak of its deuterated components. For unidentified AA metabolites, such observed differences (and/or similarities) can lend valuable insight regarding their production pathways, and we therefore now briefly review how eicosanoids are synthesized from AA. Action by the enzyme prostaglandin H synthase (also known as cyclooxygenase or COX) on AA is the first step in all prostaglandin biosynthesis. COX first abstracts one hydrogen atom from the C-13 of AA (refer to Fig. 1*C*) to form an arachidonate radical, which then reacts sequentially with two oxygen molecules, first creating an endoperoxide between C-9 and C-11 and then forming a hydroperoxide at C-15, thus forming the intermediate prostaglandin G_2. Next, COX acts as a peroxidase on prostaglandin G_2, reducing its C-15 hydroperoxide to a hydroxyl group, forming PGH_2 (22, 23). PGH_2 can then serve as

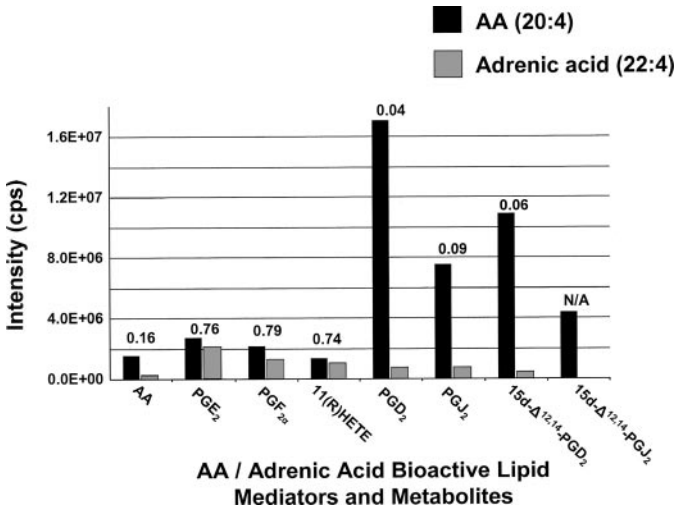

FIGURE 7. **Semi-quantitative comparison of AA, adrenic acid, and their metabolites obtained from Kdo_2-Lipid A-stimulated RAW cells.** Full-scan mass spectra obtained for AA, adrenic acid, and their metabolites permitted a semi-quantitative comparison of these species (refer to text for more detail regarding this measurement). The *number* above each pair is the ratio of adrenic acid to AA (metabolites). It should be noted that no dihomo-15d-$\Delta^{12,14}$-PGJ_2 was observed.

a substrate for a number of downstream enzymes: PGD_2 isomerase, PGE_2 isomerase, $PGF_{2\alpha}$ reductase, thromboxane synthase, or prostacyclin synthase. This leads us to conclude that the different deuterated profiles we observe for PGD_2 and PGE_2 compared with $PGF2_\alpha$ and 11(*R*)-HETE are the result of processes that occur *after* the synthesis of PGH_2, *i.e.* due to the action of downstream enzymes.

Observing the deuterated peak pattern in the full scan mass spectrum of the unidentified compound our software recognized at *m/z* 381, LC-RT 6.5 m (Fig. 5, *A* and *B*) with $([M+d_8]-H)^-$ being the most intense peak of its deuterated components suggested this compound to be more similar to $PGF_{2\alpha}$ and 11(*R*)-HETE than to PGD_2 or PGE_2. This would indicate this compound does not contain a cyclopentane keto-group as seen in PGE_2 and PGD_2 (also observed in the enzymatic and non-enzymatic products of PGD_2). As stated earlier, the MS/MS fragments observed at 363, 345, and 327 (Fig. *5C*) suggest the loss of 1-, 2-, and 3-hydroxyl groups, respectively. The most abundant MS/MS fragment at 337, 44 atomic mass units less than the parent ion mass, is a peak that is very characteristic of $PGF_{2\alpha}$ involving a charge-site remote loss of C_2H_4O from its cyclopentane ring (24). Another very abundant $PGF_{2\alpha}$ fragment occurs at 193, a 160-atomic mass unit loss resulting from the charge-site remote loss of 44 atomic mass units described above, accompanied by the loss of the methyl terminus side chain and cleaving of the bond between C-13 and C-14 ($C_7H_{16}O$) (2, 24). A 160-atomic mass unit loss from 381 results in a fragment at 221, strongly evident in Fig. *5C*. These pronounced similarities between $PGF_{2\alpha}$ and the 381 unknown, as well as their 28-atomic mass unit mass difference, led us to believe this unknown was $PGF_{2\alpha}$ with a C_2H_4 attachment at the molecule's carboxyl end, such a molecule describes 1*a*,1*b*-dihomo-9*S*,11*R*,15*S*-trihydroxy-5*Z*,13*E*-prostadienoic acid (dihomo-$PGF_{2\alpha}$). Agreement in LC-RT and MS/MS fragmentation with a dihomo-$PGF_{2\alpha}$ standard confirmed this to be the case. Structural determination for some of the unknowns listed in Table 1 (*i.e.* UNK 335-1 and UNK 353-1) will require additional experimental approaches.

Detection of Arachidonate-derived Dihomoprostaglandins—In addition to dihomo-$PGF_{2\alpha}$, a number of other dihomoprostaglandins were observed to be produced by the Kdo_2-Lipid A-stimulated cells. The tentative identities of these other dihomoprostaglandins (listed in Table 1) were determined using (i) standards when available, (ii) estimation of the increased LC-RT that results from the additional C_2H_4 attachment (actual LC-RT values were obtained using $PGF_{2\alpha}$/dihomo-$PGF_{2\alpha}$ and PGE_1/dihomo-PGE_1 standards, and these were used to extrapolate for the other compounds), and (iii) MS/MS fragmentation patterns. To correlate the LC-RT of the dihomoprostaglandins with their corresponding AA-generated counterparts, an entirely linear LC gradient was employed; this was done to avoid inconsistencies that might occur due to abrupt ramps in buffer during an LC run. The MS/MS fragmentation spectra also confirmed that the elongation of AA occurs at the carboxyl end of the molecule which, from a biosynthetic perspective, is expected. These COX products of adrenic acid (7*Z*,10*Z*,13*Z*,16*Z*-docosatetraenoic acid) appear to result from the two-carbon elongation of AA prior to the esterification of the adrenic acid to the *sn*-2 position of the cell membrane glycerophospholipid pool. This is strongly suggested by the observation of deuterated adrenic acid and dihomoprostaglandins, which originate from the supplemented AA-d_8. along with non-deuterated adrenic acid dihomologue prostaglandins produced from the endogenous AA (Fig. 6, *A* and *B*). These findings demonstrate some additional utility of the DIMPLES/MS methodology. The proposed steps in the AA elongation process, and the subsequent production of dihomoprostaglandins by stimulated cells, are depicted in Fig. 8. It should be noted that neither dinor (18 carbons), tetranor (16 carbons), nor tetrahomo (24 carbons) prostaglandins were observed to be produced by the stimulated RAW cells. Although it has been observed previously that adrenic acid added to cells can serve as a COX substrate resulting in the production of dihomoprostaglandins (15–17), there has been no demonstration of its formation *de novo* from an arachidonate precursor. As such, the question arises as to *why the elongation of AA occurs*. The addition of adrenic acid to cell culture was found previously to inhibit the conversion of AA to prostaglandins (25). It is possible, therefore, that the elongation process occurs as a regulatory mechanism, a means of limiting the production of AA derived prostaglandins? Additionally, the dihomoprostaglandins may have direct actions of their own and further investigation of these actions is warranted.

It is also possible that the 2-carbon elongation may be taking place on the already formed 20-carbon prostaglandins; however, the observation of AA-generated adrenic acid (Fig. 6*A*) raises some doubts about this scenario. Additionally, the observed plentiful generation of some dihomoprostaglandins compared with the meager production of others (discussed in more detail below), raises further questions regarding a prostaglandin two-carbon elongation scheme. The action of an elongase should be fairly non-discriminatory considering its broad, nonspecific class of action. As such, if the elongase was

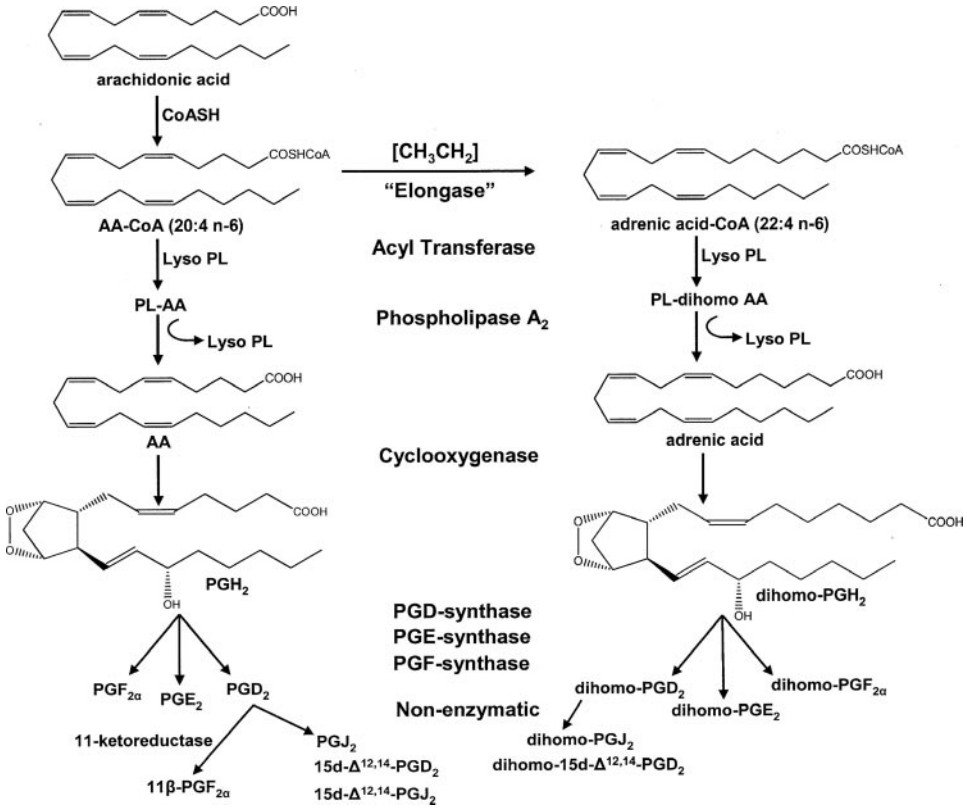

FIGURE 8. **Proposed steps in the two-carbon elongation of AA and the subsequent production of dihomoprostaglandins.** Proposed steps in the AA elongation process, and the subsequent production of dihomoprostaglandins derived from adrenic acid by Kdo_2-Lipid A-stimulated cells are shown. Compared with the AA-derived products, note the absence of both the non-enzymatic breakdown product dihomo-15d-$\Delta^{12,14}$-PGJ_2 and the PGD_2 enzymatic product dihomo-11β-$PGF_{2\alpha}$.

acting on the prostaglandins one would expect to observe all the dihomoprostaglandins being produced in amounts that follow their 20-carbon counterparts (*i.e.* PGD_2 is the prostaglandin produced in most abundance and, therefore, dihomo-PGD_2 should be the most abundantly observed dihomoprostaglandin). The higher selectivity of the prostaglandin synthases can explain the observed discrepancy in dihomoprostaglandin production (discussed below) and supports an elongation scheme as depicted in Fig. 8.

As mentioned briefly above, it is interesting to note the observed production of certain dihomoprostaglandins, including their relative amounts or, interestingly, their absences. The dihomoprostaglandins observed to be produced by the Kdo_2-Lipid A stimulated RAW cells are dihomo-(PGE_2, PGD_2, $PGF_{2\alpha}$, 11(*R*)-HETE, PGJ_2, and 15d-$\Delta^{12,14}$-PGD_2). It is worth noting differences in the relative abundance of some prostaglandins/dihomoprostaglandins, for example PGD_2 *versus* PGE_2 and dihomo-PGD_2 *versus* dihomo-PGE_2 (Fig. 7).

Specificity Differences for PGD-synthase Acting on Dihomo-PGH_2—PGD_2 is by far the most abundant observed AA-derived product generated by the Kdo_2-Lipid A-stimulated cells; typically 5- to 10-fold higher in intensity than PGE_2 (Fig. 7). Dihomo-PGE_2 is roughly 3-fold higher than dihomo-PGD_2. The noticeable decrease in dihomo-PGD_2 production is also supported by the observed lower production of its non-enzymatic breakdown products dihomo-PGJ_2 and dihomo-15d-$\Delta^{12,14}$-PGD_2. This implies that adrenic acid may be a particularly poor substrate for PGD-synthase or adrenic acid may be a particularly good substrate for PGE- and PGF-synthase. This is supported by the observation that, although adrenic acid is observed at ≈0.16 the amount of AA, dihomo-PGE_2 and dihomo-$PGF_{2\alpha}$ are ≈0.8 the amount of PGE_2 and $PGF_{2\alpha}$, respectively. Production of the non-enzymatic PGD_2 breakdown product dihomo-15d-$\Delta^{12,14}$-PGJ_2 and the enzymatic product dihomo-11β-$PGF_{2\alpha}$ were notably absent. This absence of dihomo-15d-$\Delta^{12,14}$-PGJ_2 is of particular interest, because 15d-$\Delta^{12,14}$-PGJ_2 and its role as an endogenous high-affinity ligand for the peroxisome proliferator-activated receptor γ have been the topic of much current discussion and controversy (26–29). If dihomo-15d-$\Delta^{12,14}$-PGJ_2 is strictly a simple non-enzymatic breakdown product of dihomo-PGD_2, as 15d-$\Delta^{12,14}$-PGJ_2 is assumed to be of PGD_2, might we expect to observe its presence along with dihomo-PGJ_2 and dihomo-15d-$\Delta^{12,14}$-PGD_2? Its absence in these studies suggests that its production may be more involved than simple non-enzymatic breakdown. Additional experiments are planned to conduct absolute quantitative measurements of the dihomoprostaglandins and investigate further the notable absence of dihomo-15d-$\Delta^{12,14}$-PGJ_2. Investigating the elongation and analog prostaglandin production of other supplemented fatty acids, particularly eicosapentaenoic acid (20:5(*n*-3)) and docosahexaenoic acid (22:6(*n*-3)), should now be possible using these methods.

Acknowledgments—We express our sincere gratitude to Drs. Michel Lagarde (National University of Applied Science, Lyon, France) and Robert C. Murphy (University of Colorado School of Medicine, Denver, CO), and to Raymond Deems of our laboratory, for their helpful discussions involving this work.

REFERENCES

1. Bergstrom, B., and Samuelsson, B. (1962) *J. Biol. Chem.* **237,** 3005–3006
2. Murphy, R. C., Barkley, R. M., Zemski Berry, K., Hankin, J., Harrison, K., Johnson, C., Krank, J., McAnoy, A., Uhlson, C., and Zarini, S. (2005) *Anal. Biochem.* **246,** 1–42
3. Fischer, C., and Frohlich, J. C. (1982) *Adv. Lipid Res.* **19,** 185–202
4. Margalit, A., Duffin, K. L., and Isakson, P. C. (1996) *Anal. Biochem.* **235,** 73–81
5. Kempen, E. C., Yang, P., Felix, E., Madden, T., and Newman, R. A. (2001) *Anal. Biochem.* **297,** 183–190
6. Takabatake, M., Hishinuma, T., Suzaki, N., Chiba, S., Tsukamoto, H., Nakamura, H., Saga, T., Tomioka, Y., Kurose, A., Sawai, T., and Mizugaki, M. (2002) *Prostaglandins Leukot. Essent. Fatty Acids* **67,** 51–56

7. Yang, P., Felix, E., Madden, T., Fischer, S. M., and Newman, R. A. (2002) *Anal. Biochem.* **308,** 168–177
8. Nithipatikom, K., Laabs, N. D., Isbell, M. A., and Campbell, W. B. (2003) *J. Chromatogr. B* **785,** 135–145
9. Kingsley, P. J., Rouzer, C. A., Saleh, S., and Marnett, L. J. (2005) *Anal. Biochem.* **343,** 203–211
10. Kita, Y., Takahashi, T., Uozumi, N., Nallan, L., Gelb, M. H., and Shimizu, T. (2005) *Biophys. Res. Commun.* **330,** 898–906
11. Kita, Y., Takahashi, T., Uozumi, and Shimizu, T. (2005) *Anal. Biochem.* **342,** 134–143
12. Lu, Y., Hong, S., Tjonanhen, E., and Serhan, C. N. (2005) *J. Lipid Res.* **46,** 790–802
13. Aderem, A. (2005) *Cell* **121,** 511–513
14. Raetz, C. R. H., Garrett, T. A., Reynolds, C. M., Shaw, W. A., Moore, J. D., Smith, D. C., Riberio, A. A., Murphy, R. C., Ulevitch, R. J., Fearns, C., Reichart, D., Glass, C. K., Benner, C., Subramaniam, S., Harkewicz, R., Bowers-Gentry, R. C., Buczynski, M. W., Cooper, J. A., Deems, R. A., and Dennis, E. A. (2005) *J. Lipid Res.* **46,** 969–976
15. Sprecher, H., VanRollins, M., Sun, F., Wyche, A., and Needleman, P. (1982) *J. Biol. Chem.* **257,** 3912–3918
16. Cagen, L. M., Zusman, R. M., and Pisano, J. J. (1979) *Prostaglandins* **18,** 617–621
17. Campbell, W. B., Falck, J. R., Okita, J. R., Johnson, A. R., and Callahan, K. S. (1985) *Biochim. Biophys. Acta* **837,** 67–76
18. Pedrioli, P. G. A., Eng, J. K., Hubley, R., Vogelzang, M., Deutsch, E. W., Raught, B., Pratt, B., Nilsson, E., Angeletti, R., Apweiler, R., Cheung, K., Costello, C. E., Hermjakob, H., Huang, S., Julian, R. K., Jr., Kapp, E., McComb, M. E., Oliver, S. G., Omenn, G., Paton, N. W., Simpson, R., Smith, R., Taylor, C. F., Zhu, W., and Aebersold, R. A. (2004) *Nat. Biotechnol.* **22,** 1459–1466
19. Lee, S. H., Williams, M. V., and Blair, I. A. (2005) *Prostaglandins Other Lipid Mediat.* **77,** 141–157
20. Fahy, E., Subramaniam, S., Brown, H. A., Glass, C. K., Murphy, R. C., Merrill, A. H., Raetz, C. R. H., Russell, D. W., Seyama, Y., Shaw, W., Shimizu, T., Spener, F., van Meer, G., VanNieuwenhze, M. S., White, S. H., Witztum, J. L., and Dennis, E. A. (2005) *J. Lipid Res.* **46,** 839–862
21. Wantanabe, K. (2002) *Other Lipid Mediat.* **68–69,** 401–407
22. Morita, I. (2002) *Prostaglandins Other Lipid Mediat.* **68–69,** 165–175
23. Smith, W. L., and Song, I. (2002) *Prostaglandins Other Lipid Mediat.* **68–69,** 115–128
24. Zirrolli, J. A., Davoli, E., Bettazzoli, L., Gross, M. L., and Murphy, R. C. (1990) *J. Am. Soc. Mass Spectrom.* **1,** 325–335
25. Cagen, L. M., and Baer, P. G. (1980) *Life Sci.* **26,** 765–770
26. Forman, B. M., Tontonoz, P., Chen, J., Brun, R. P., Spiegelman, B. M., and Evans, R. M. (1995) *Cell* **83,** 803–812
27. Straus, D. S., Pascual, G., Li, M., Welch, J. S., Ricote, M., Hsiang, C.-H., Sengchanthalangsy, L. L., Ghosh, G., and Glass, C. K. (2000) *Proc. Natl. Acad. Sci. U. S. A.* **97,** 4844–4849
28. Bell-Parikh, L. C., Ide, T., Lawson, J. A., McNamara, P., Reilly, M., and FitzGerald, G. A. (2003) *J. Clin. Invest.* **112,** 945–955
29. Powell, W. S. (2003) *J. Clin. Invest.* **112,** 828–830

Arachidonate-derived Dihomoprostaglandin Production Observed in Endotoxin-stimulated Macrophage-like Cells

Richard Harkewicz, Eoin Fahy, Alexander Andreyev and Edward A. Dennis

J. Biol. Chem. 2007, 282:2899-2910.
doi: 10.1074/jbc.M610067200 originally published online November 29, 2006

ADDITIONS AND CORRECTIONS

This paper is available online at www.jbc.org

THE JOURNAL OF BIOLOGICAL CHEMISTRY VOL. 282, NO. 39, p. 29068, September 28, 2007

VOLUME 280 (2005) PAGES 2405–2408

VE-cadherin links tRNA synthetase cytokine to anti-angiogenic function.

Eleni Tzima, John S. Reader, Mohamad Irani-Tehrani, Karla L. Ewalt, Martin A. Schwartz, and Paul Schimmel

PAGE 2406:

Fig. 1: The incorrect images were printed for *panels a* and *b*. The correct images are shown below.

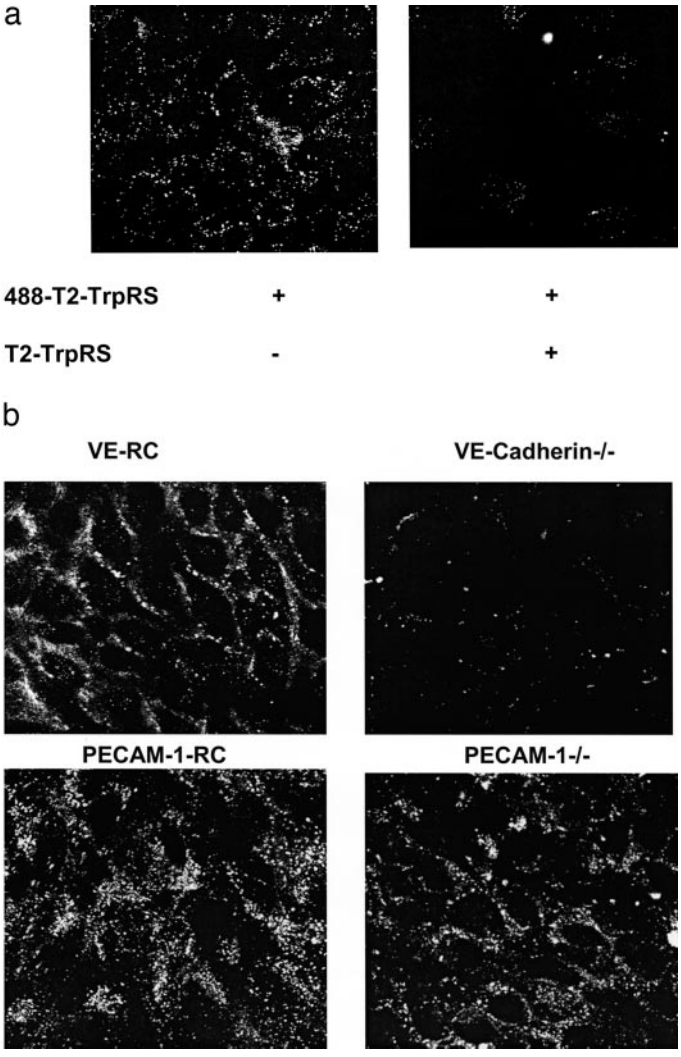

FIGURE 1. *Panels a* and *b*.

VOLUME 282 (2007) PAGES 2899–2910

Arachidonate-derived dihomoprostaglandin production observed in endotoxin-stimulated macrophage-like cells.

Richard Harkewicz, Eoin Fahy, Alexander Andreyev, and Edward A. Dennis

PAGE 2910:

Although the authors are listed correctly, Ref. 14 refers to the incorrect paper in *J. Lipid Res*. The correct reference should read: Raetz, C. R. H., Garrett, T. A., Reynolds, C. M., Shaw, W. A., Moore, J. D., Smith, D. C., Riberio, A. A., Murphy, R. C., Ulevitch, R. J., Fearns, C., Reichart, D., Glass, C. K., Benner, C., Subramaniam, S., Harkewicz, R., Bowers-Gentry, R. C., Buczynski, M. W., Cooper, J. A., Deems, R. A., and Dennis, E. A. (2006) *J. Lipid Res*. **47,** 1097–1111.